

- SCHWEBER, S. S. (1961). *An Introduction to Relativistic Quantum Field Theory*. New York: Harper and Row.
- SCHWINGER, J. (1948). *Phys. Rev.* **73**, 407–409.
- SHULL, C. G. & YAMADA, Y. (1962). *J. Phys. Soc. Jpn*, **17**, BIII, 1–6.
- STEINSVOLL, O., SHIRANE, G., NATHANS, R., BLUME, M., ALPERIN, H. A. & PICKART, S. J. (1967). *Phys. Rev.* **161**, 499–506.
- STEPHEN, R. M. & FRAUNFELDER, H. (1965). *Polarization of Radiation Following  $\beta$ -Decay. Alpha, Beta, Gamma-ray Spectroscopy*. Edited by K. SIEGBAHN, ch. 4, pp. 1456–1465. Amsterdam: North-Holland.
- TOLHOEK, H. A. (1956). *Rev. Mod. Phys.* **28**, 277–298.
- TRAMMELL, G. T. (1953). *Phys. Rev.* **92**, 1387–1393.
- VAILLANT, F. (1977). *Acta Cryst.* **A33**, 967–970.

*Acta Cryst.* (1981). **A37**, 324–331

## Diffraction of X-rays by Magnetic Materials. II. Measurements on Antiferromagnetic $\text{Fe}_2\text{O}_3$

BY M. BRUNEL AND F. DE BERGEVIN

*Laboratoire de Cristallographie, Centre National de la Recherche Scientifique, Laboratoire associé à l'USMG, 166 X, 38042 Grenoble CEDEX, France*

(Received 31 July 1978; accepted 4 November 1980)

### Abstract

Two of the magnetic superlattice Bragg reflections of a single crystal of hematite ( $\text{Fe}_2\text{O}_3$ ) have been measured by diffraction of X-rays produced from a conventional source, and compared to the intensities expected from the photon–spin scattering. Several orientations of the spins relative to the beams have been realized by rotating the crystal and by changing its temperature through the Morin (spin-flip) transition; in some of the measurements, the polarization produced by the monochromator was enhanced and this produced a visible asymmetry in the dependence of the intensities on the spin direction. The variations of the intensities during these changes of configuration are characteristic of magnetic scattering; the observed variations, as well as the absolute intensities, agree with the theory apart from some discrepancies. These may be due to intense multiple-scattering effects, and to some possible anomalies in the spin direction near the sample surface. As an application of this technique, changes of the direction of magnetization when a magnetic field is applied to the weakly ferromagnetic room-temperature phase have been investigated.

### I. Introduction

In paper I (de Bergevin & Brunel, 1981), we have developed the general formulae for the diffraction of X-rays by a magnetic compound by taking into account the interaction between photons and spins. We have also described the experiments in which this effect is detected with ferro- and ferrimagnetic compounds.

The occurrence of antiferromagnetic ordering lowers the symmetry of a crystal, and eventually enlarges the unit cell. This generally produces in the X-ray diffraction diagram some superstructure reflections due to the photon–spin interaction (except in the cases, for example  $\text{Cr}_2\text{O}_3$ , where the symmetry centre disappears). In a previous paper (de Bergevin & Brunel, 1972), we have shown the existence of the magnetic reflections  $\frac{111}{222}$  and  $\frac{333}{222}$  in nickel oxide  $\text{NiO}$ ; these reflections disappeared at the Néel point. In order to make a complete and convincing check of the theoretical predictions we have undertaken the same type of experiments on  $\text{Fe}_2\text{O}_3$ .

In the first part of this article, we derive the principle of our measurements from the expression for the intensity of the magnetic reflections (§ II) and describe the application of this to  $\text{Fe}_2\text{O}_3$  (§ III). In the second part, after a description of our apparatus (§ IV) and of the experimental procedure (§ V), the results are given and compared to the expected ones.

### II. Principle of the experiment

In a study made with an unpolarized source, and with a monochromator diffracting in the same plane as the sample, the diffracted intensity is given by the formulae (19), (20) and (22) of paper I. The intensity of a pure superstructure reflection (without any contribution from the non-magnetic atoms) is proportional to  $|\mathbf{B} \cdot \mathbf{S}|^2$ . We assume all the spins to be collinear and define the spin-density structure factor  $\mathbf{S}(hkl)$  as in the ferromagnetic case:

$$\mathbf{S}(hkl) = \hat{\mathbf{S}}F_T(hkl)f_M(\theta)\mu/2, \quad (1)$$

where  $\hat{\mathbf{S}}$  is a unit vector parallel to the moments of the magnetic atoms,  $\mu$  the magnitude of these moments in Bohr magnetons,  $f_M(\theta)$  the unitary magnetic form factor of these atoms, and  $F_T$  the trigonometric structure factor of the magnetic arrangement.

Let  $S_x$ ,  $S_y(\psi)$ ,  $S_z(\psi)$  be the projections of  $\hat{\mathbf{S}}$  on the three axes as defined in Fig. 1 [z is perpendicular to the diffraction plane ( $\mathbf{k}_i$ ,  $\mathbf{k}_f$ )], and let  $S_y$ ,  $S_z$  depend on an angular variable  $\psi$  defined below. For a symmetrical reflection at a crystal face and an incident beam with an intensity  $I_0$ , the integrated intensity  $I(hkl)$  of a magnetic superstructure reflection is given by

$$I(hkl) = I_0 \left( \frac{\lambda^3}{\sin 2\theta} \frac{N^2}{2\mu_a} \right) \left( \frac{r_e \lambda_c}{\lambda} \right)^2 (F_T(hkl) \mu f_M(\theta))^2 \times \sin^2 \theta P(\psi), \quad (2)$$

$$P(\psi) = S_z^2(\psi) \cos^2 \theta + \sin^2 \theta \{ S_y^2(\psi) \cos^2 \theta + S_x^2 \sin^2 \theta + [\sin^2 2\alpha / (1 + \cos^2 2\alpha)] \times S_x S_y(\psi) \sin 2\theta \}.$$

The factor  $(\lambda^3/\sin 2\theta) (N^2/2\mu_a)$  takes into account the Lorentz factor, the absorption  $\mu_a$ , the number of cells per unit volume  $N$ , and  $\alpha$  is the Bragg angle of the monochromator.

If the sample is rotated around the scattering vector ( $x$  axis) by an angle  $\psi$  from a reference position, the reciprocal-lattice point  $hkl$  stays on the Ewald sphere (Fig. 2);  $\theta$ ,  $F_T(hkl)$  and the absorption do not vary since the beam is symmetrically reflected at a crystal face, however the  $\hat{\mathbf{S}}$  direction moves and  $S_y$  and  $S_z$  are

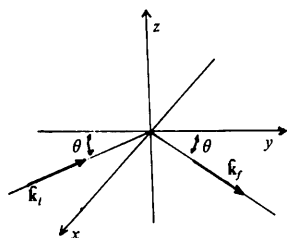


Fig. 1. Definition of the  $x, y, z$  axes.  $z$  is perpendicular to the diffraction plane.

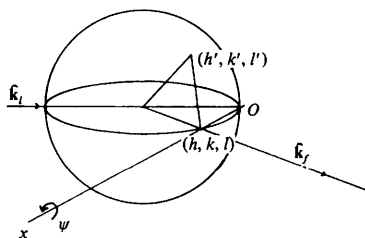


Fig. 2. Principle of the experiments. For  $\psi$  rotation around  $x$ , the  $hkl$  reflection remains on the Ewald sphere, while other reciprocal-lattice points  $h'k'l'$  go through it.

changed. In the case of a uniaxial crystal for which there is a unique spin direction,  $S_y$  and  $S_z$  are simple functions of  $\psi$ ; if several spin directions are possible and the crystal is not a single domain, the mean values of  $S_x^2$ ,  $S_y^2(\psi)$ ,  $S_z^2(\psi)$  and  $S_x S_y(\psi)$  for the different domains have to be introduced in relation (2).

### III. Application to $\text{Fe}_2\text{O}_3$

In the NiO crystal studied previously (de Bergevin & Brunel, 1972), 12 kinds of magnetic domains with different  $\hat{\mathbf{S}}$  orientations were simultaneously present. This number can be reduced to three because the four  $T$  domains can be coalesced to one by pressing upon an annealed crystal, but it is very difficult to obtain a single-domain crystal. Therefore the intensities of the  $\frac{1}{2}\frac{1}{2}\frac{1}{2}$  and  $\frac{3}{2}\frac{3}{2}\frac{3}{2}$  reflections are constant for all the angles  $\psi$  since an average over the three domains gives  $S_z^2 = S_y^2 = \frac{1}{2}$  and  $S_x^2 = 0$  [the spins lie in the (111) plane]. Even for a suitably chosen  $hkl$  reflection, the existence of the domains will reduce the variations of  $P(\psi)$ .

Corundum  $\text{Fe}_2\text{O}_3$  does not have this inconvenience. At temperatures below  $T_N = 948\text{K}$  the iron magnetic moments are antiferromagnetically ordered; they are parallel within any (001)\* plane and two adjacent planes are antiferromagnetically coupled. The magnetic cell is identical to the chemical cell and the effect of the magnetic order is only to suppress the  $c/2$  translation between the  $\text{Fe}^{3+}$  ions (Fig. 3) (this translation does not apply to the oxygen ions, which are not on a glide plane of the  $R\bar{3}c$  space group). This peculiarity was used by Nathans, Pickart, Alperin & Brown (1964) to make polarized neutron measurements; we shall see later that it is a very important inconvenience for our experiments. For temperatures  $T < T_M$  with  $T_M$  the Morin temperature  $\approx 253\text{K}$ , the spins are along the [001] axis (Shull, Strauser & Wollan, 1951) (Fig. 4). For  $T_M < T < T_N$  the spins are within the (001) plane but not exactly antiparallel, which gives a weak ferromagnetic moment lying in the (001) plane (Dzialoshinsky, 1958); we neglect this effect and apply (1). Since it is difficult in our experimental set up to reach temperatures above the Néel point, we compare the theoretical expressions with the intensity of the magnetic reflections measured above and below the Morin transition only.

In the low-temperature phase the crystal has a single spin direction and there are two types of antiphase domains which cannot be distinguished. In the high-temperature phase ( $T > T_M$ ) the spins can be ordered along one of three directions, interchanged by the threefold axis. We shall suppose, at least in the first part of this work, that the three kinds of domains (as stated above we do not distinguish domains of the same

\* Indices are referred to the hexagonal cell ( $a = 5.038$  and  $c = 13.772 \text{ \AA}$ ).

antiphase pair), in the absence of an external magnetic field, occur with the same probability and are homogeneously distributed in the crystal (Nathans *et al.*, 1964).

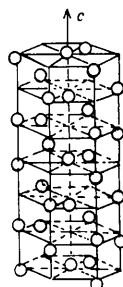


Fig. 3.  $\text{Fe}^{3+}$  ions in  $\text{Fe}_2\text{O}_3$ . Spins within a (001) plane are parallel. Two adjacent (001) planes are coupled antiferromagnetically.

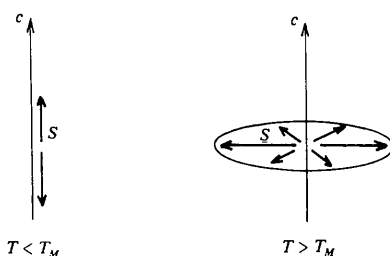


Fig. 4. Changes in the spin direction at the Morin transition.

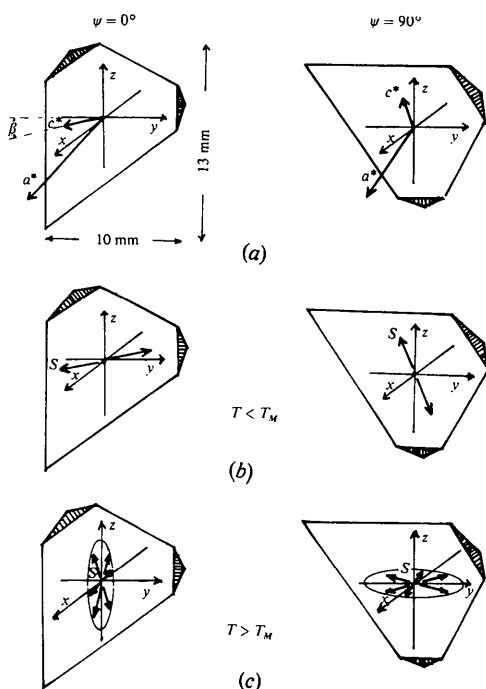


Fig. 5. Direction of (a) the reciprocal axes, (b) the spins at low temperature, (c) the spins at room temperature. They are related to the  $x, y, z$  axes and drawn for the crystal position  $\psi = 0^\circ$  and  $\psi = 90^\circ$ .

In order to increase the intensity of the magnetic Bragg reflection, and to avoid absorption correction, the measurements are made on a large plate in symmetrical reflection. The crystal is cut parallel to the chosen Bragg plane. The choice of this plane is imposed by the following requirements: (1) the reflections of pure magnetic origin are of the type  $h0l$  with  $l = 2n + 1$ ; (2) in order to maximize the variations of  $P(\psi)$  on  $\psi$  one must have the  $c$  axis as near as possible to the reflection plane; (3) in order to reinforce the intensity one must have a high value of  $F$ , which is realized for  $l = 1$  or  $3$ . The planes (303) and (101), which make an angle  $\beta = 17^\circ$  with the  $c$  axis, meet these requirements.

If the reference position  $\psi = 0$  is taken for  $c$  (or reciprocal  $c^*$ ) in the diffraction plane  $xy$  (Fig. 5), and if  $\psi$  is the rotation angle around the scattering vector from this position, the intensities are given by making the following replacements in  $P(\psi)$ :

– for  $T < T_M$  (spins along the  $c$  axis) one introduces in (2) the values:

$$\begin{aligned} S_x^2 &= \sin^2 \beta \\ S_y^2 &= \cos^2 \beta \cos^2 \psi \\ S_z^2 &= \cos^2 \beta \sin^2 \psi \\ S_x S_y &= -\sin \beta \cos \beta \cos \psi. \end{aligned} \quad (3)$$

When the  $\theta$  angle is not too high, as is the case in our measurements (for the 303 reflection  $\theta = 34^\circ$  with  $\text{Cu } K\alpha$ ), the term  $S_z^2 \cos^2 \theta$  is preponderant in (2) and the intensity of the reflection at low temperature is maximum for  $\psi = 90^\circ$  and minimum for  $\psi = 0^\circ$ .

– for  $T > T_M$  the spins lie in the (001) plane; in zero magnetic field one expects them to be equally distributed along three directions in this plane. The terms  $S_x^2$ ,  $S_y^2$ ,  $S_z^2$  and  $S_x S_y$  in (2) are the averages over these three domains:

$$\begin{aligned} S_x^2 &= \cos^2 \beta / 2 \\ S_y^2 &= (\sin^2 \psi + \sin^2 \beta \cos^2 \psi) / 2 \\ S_z^2 &= (\cos^2 \psi + \sin^2 \beta \sin^2 \psi) / 2 \\ S_x S_y &= (\sin \beta \cos \beta \cos \psi) / 2. \end{aligned} \quad (4)$$

The intensity of 303 in the high-temperature phase is then maximum for  $\psi = 0^\circ$  and minimum for  $\psi = 90^\circ$ .  $P(\psi)$  ( $T < T_M$ ) increases whereas  $P(\psi)$  ( $T > T_M$ ) decreases (Fig. 9) and the ratio

$$R(\psi) = P(\psi) (T < T_M) / P(\psi) (T > T_M)$$

varies drastically, from  $R(0) = 0.5$  to  $R(90) = 3.5$  for 303 (Fig. 10).

With the usual setting of the monochromator we have

$$\sin^2 2\alpha / (1 + \cos^2 2\alpha) \simeq 0.1,$$

the cross term in  $S_x S_y$  of the relation (2) is weak and  $I(\psi)$  is symmetrical with respect to  $\psi = 90^\circ$ .

#### IV. Apparatus

The experiments have been made with either Cu  $K\alpha$  or Co  $K\alpha$  radiation. Though the compound  $\text{Fe}_2\text{O}_3$  is favourable [ $\mu = 5\mu_B$  in (1)], the intensity remains very weak due to the factor  $(\lambda_c/\lambda) \simeq 2 \times 10^{-4}$ .

We have used (Fig. 6) a powder goniometer upon which an Euler circle supports the rotation axis of a goniometer head: this is the  $\psi$  axis whose rotation has been automated with a stepping motor. An oriented graphite monochromator placed between the sample and the detector eliminates the continuous spectrum and the fluorescence of iron; however, it transmits the  $\lambda/2$  radiation whose Thomson reflections are superposed on the weak magnetic ones of  $\lambda$  radiation. Several methods have been tried in attempts to reduce the rate of the harmonics: lowering of the excitation of the tube, monochromatization by the 111 reflection of germanium, use of a solid-state detector. The best result, in respect of both transmission of  $\lambda$  and elimination of  $\lambda/2$  was obtained by the total reflection of the incident beam at a mirror.

The mirror is cut from a good quality glass plate and covered, by evaporation in vacuum, with a thin layer of nickel. It is placed in a press which gives it an adjustable curvature; an approximate focusing is thus allowed when the system is placed at the window of the X-ray tube. The path of the X-ray beam being lengthened by about 400 mm, the whole system is placed in vacuum; this avoids both absorption by air and oxidation of the nickel layer in the X-ray beam. The sample-detector path is also put in vacuum. After reflection by the mirror, the beam is very slightly divergent; this is the main limitation in the intensity, which is nevertheless increased by a ratio of about 7 to 8 compared with previous experiments (de Bergevin & Brunel, 1972) where the lowering of the voltage was used.

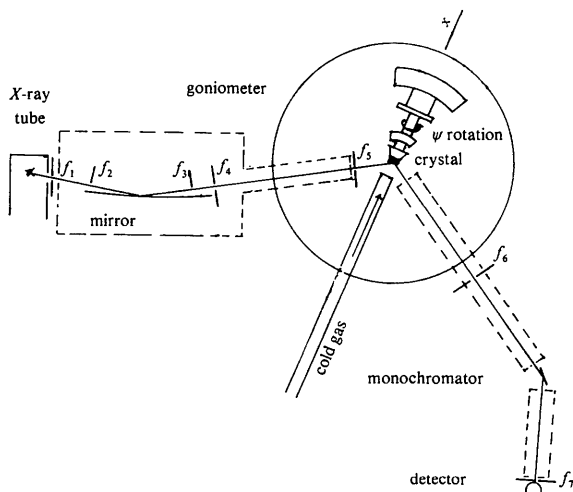


Fig. 6. Sketch of the apparatus.

The temperature of the crystals, below the Morin transition, is controlled by a stream of cold gas. Because of the large dimensions of the crystal ( $\sim 10$  mm) a flow of 30–40 l/minute is necessary. Such a flow would be obtained at the expense of a prohibitive liquid-nitrogen consumption, if the gas were produced by evaporation of the liquid itself. We used instead a dried air stream cooled by going through a heat exchanger immersed in a liquid-nitrogen tank, and then warmed to the desired temperature by mixing with room-temperature air.

#### V. Experimental procedure

Many small plates were cut from a natural crystal (Elba crystal), and were discarded because they presented many faults at their surface. We used instead a large synthetic crystal supplied by Crystal-Tec. This crystal gave a Morin transition  $T_M$  of about 258 K which indicated a very low concentration of impurities (Flanders & Remeika, 1964).

##### Multiple diffraction effects

The superstructure reflections  $hkl$  in which we are interested are forbidden reflections of the  $R3c$  space group, but during a rotation around the scattering vector, other reciprocal-space points, occupied by Thomson reflections, will go through the Ewald sphere. Let us suppose that  $h'k'l'$  are the indices of such a point (Fig. 2). If the  $h''k''l''$  ( $h'' = h - h'$ ,  $k'' = k - k'$ ,  $l'' = l - l'$ ) reflection is allowed, a reflection due to the double diffraction (Renninger) effect will appear superimposed on the magnetic reflection.\* To determine the  $\psi$  positions of these reflections, we have used a method developed by Cole, Chambers & Dunn (1962) for a germanium crystal. A computer program gave the positions of the 540 reflections that enter into a detector for a  $360^\circ$  rotation at the position of the 303 magnetic reflections with Cu  $K\alpha$ . This number is about 300 for the 303 and the 101 studied with Co  $K\alpha$ . The  $\psi = 0$  position of the crystal has been determined exactly by using the indexing and the symmetries of the multiple-reflection spectrum.

Some of these multiple-diffraction reflections are  $10^3$  or  $10^4$  times more intense than the magnetic ones. Their large width is due to the vertical divergence of the beam and it depends on their position on the Ewald sphere. These multiple diffraction effects are the main source of difficulties and errors in our measurements. Fortunately the reflections are in general not uniformly distributed

\* This problem does not exist when the chemical and the magnetic cells are different, as in NiO. In this case, two Thomson reflections cannot give double diffraction superimposed on the magnetic reflection.

in  $\psi$  and it was possible to measure the magnetic reflections in some positions.

### Method of measurement

The crystal was set on the Thomson reflection position. However, for these reflections, the  $I(\psi)$  intensity is never totally constant during a  $\psi$  rotation (owing to crystalline quality and imperfect setting), so that it is necessary to reset the crystal for every  $\psi$  position chosen for a measurement. When the goniometer goes from one reflection to another, by a  $\theta-2\theta$  rotation and with a fixed  $\psi$  angle, no reset is necessary, which allows one to keep the same setting for measuring the superstructure reflection; this is described by a  $\theta-2\theta$  scan, step-by-step, with a step of  $1/100$  degree in  $\theta$ .

The effect of the variations of the generator power is reduced by oscillating many times (between 10 and 50) around the reflection. The counting time is one minute per step so that the time of measurement of one reflection is between 8 and 40 h. The results, collected on punched tape, are summed up by a computer in order to obtain the intensity  $I(hkl)$  of the magnetic superstructure reflection. The slow variations of the incident beam are corrected by measuring before and after every experiment the intensity of one or two Thomson reflections. From these intensities we obtain the intensity  $I_0$  of the incident beam and, placing this value in (2), we calculate the  $I(\psi)$  function; in these calculations we use the atomic positions given by Blake, Hessewicks, Zoltai & Finger (1966) and the values of  $f_M(\theta)$  determined by Brockhouse, Corliss & Hastings (1955) by neutron diffraction. The determination of  $I_0$  is valid only when the extinction effects are not too large. This is almost certainly true for the 202 and 404 reflections because they are very weak.

For every  $\psi$  position of the crystal, we have measured  $P(\psi)$  at 183 and 298 K, under and above the Morin transition and far enough from it in order to be sure that only one phase was present in the crystal. No thermal corrections have been made. Problems could come from some change, when the temperature is lowered, of the intensities of the two weak Thomson reflections used for the normalization. Blake *et al.* (1966) give for  $\text{Fe}_2\text{O}_3$  an isotropic temperature factor  $B_{\text{Fe}} = 0.48$  for iron and  $B_{\text{O}} = 0.49$  for oxygen at room temperature. Nevertheless if we suppose, for example, that  $\bar{B}$  changes from 0.49 to 0.25 or  $B_{\text{O}}$  from 0.49 to 0.25 (with  $B_{\text{Fe}}$  constant) or  $B_{\text{Fe}}$  from 0.48 to 0.25 (with  $B_{\text{O}}$  constant), the calculated variation of  $I(202)$  never exceeds 6%.

## VI. Results

In Fig. 7, we have reproduced the experimental profile of the magnetic reflection 303 [at  $\lambda \text{ Co } K\alpha$ ] for two  $\psi$

angles. The intensity is very much higher than the one measured in NiO in the preceding paper (de Bergevin & Brunel, 1972). For instance 200 counts  $\text{min}^{-1}$  at the top of the 303 reflection are to be compared with 2 counts  $\text{min}^{-1}$  in NiO.

We have (1) measured the variations of  $I(303)$  as a function of  $\psi$ , (2) showed that the cross term  $S_x S_y$  produces a measurable asymmetry in  $P(\psi)$  for this reflection, and (3) measured the variation of  $I(101)$  as a function of  $\psi$ .

(1) The variations of  $I(303)$  as a function of  $\psi$  have been studied with  $\text{Cu } K\alpha$  radiation. Because of the Renninger effect, we have been able to measure  $I(303)$  in only five  $\psi$  positions ( $0 < \psi < 90^\circ$ ). The intensity of 303 changes when the temperature is lowered from 298 to 183 K because of the change of orientation of the magnetic moments. On the other hand,  $I(303)$  changes notably, at a fixed temperature, when the crystal is rotated around the scattering vector (Fig. 7). At 298 K  $> T_M$ , the integrated intensity varies from 0.38 at  $\psi = 6^\circ$  to 0.21 at  $\psi = 73^\circ$ . At 183 K  $< T_M$ , it varies from 0.21 at  $\psi = 6^\circ$  to 0.56 at  $\psi = 73^\circ$  (at the position  $\psi = 0$ , the hexagonal  $c$  axis lies in the diffraction plane).

Fig. 8 shows the experimental results  $P(\psi)$  at these temperatures, compared to the theoretical ones. The

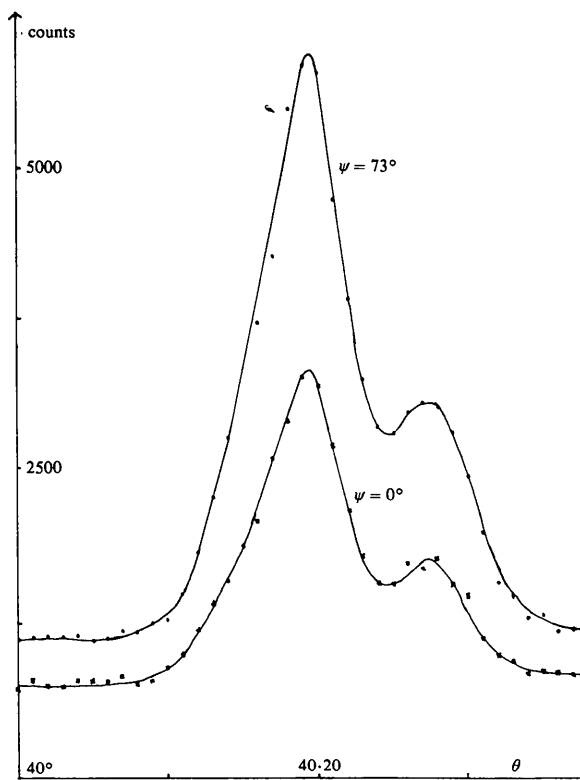


Fig. 7. The 303 magnetic superlattice reflection at low temperature ( $T < T_M$ ) for  $\psi = 0$  and  $\psi = 73^\circ$  (we have not determined the reason why the background is weaker for  $\psi = 0$ ).  $\text{Co } K\alpha$  radiation; 1100 W; 20 min/point.

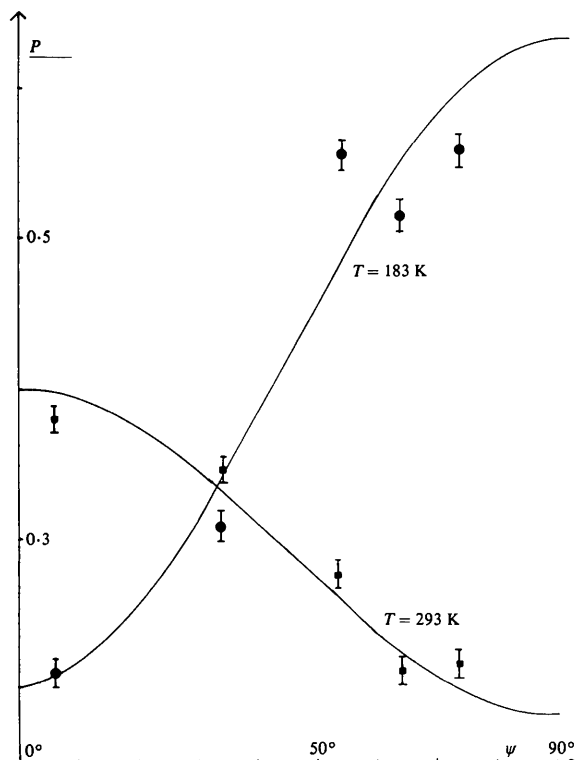


Fig. 8. Experimental values of  $P(\psi)$  at low and room temperatures (303 reflection and  $\text{Cu } K\alpha$  radiation). The continuous lines represent the calculated functions  $P(\psi)$ .

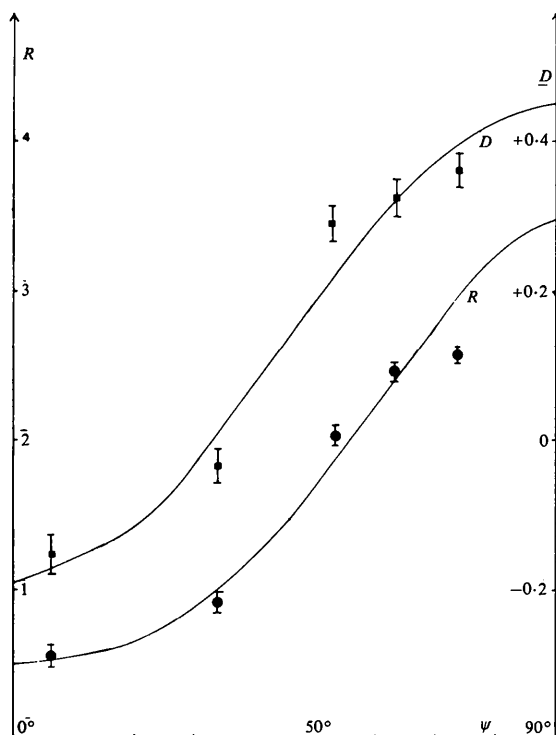


Fig. 9. Experimental values of  $R(\psi)$  and  $D(\psi)$  (303 magnetic reflection). The continuous lines represent the calculated functions.

cross term  $S_x S_y$  has been neglected in the calculation because it is small when the radiation used is  $\text{Cu } K\alpha$  monochromatized by the 002 reflection of graphite (see the end of § III). The experimental values of  $P(\psi)$  agree with the theoretical ones, though some of them differ by more than the statistical errors. Other errors may be due to extinction problems or to multiple-diffraction effects. As an attempt to eliminate these errors, we have reported in Fig. 9 the change in the ratio  $R(\psi) = I(\psi, 183 \text{ K})/I(\psi, 298 \text{ K})$  independent of  $I_0$  and the change in the difference  $D(\psi) = P(\psi, 183 \text{ K}) - P(\psi, 298 \text{ K})$  independent of Renninger effects. The agreement between experimental and theoretical curves  $R(\psi)$  and  $D(\psi)$  is of the same order of magnitude as for  $P(\psi)$  curves.

The agreement between the observed and calculated variations of  $R(\psi)$  and  $D(\psi)$  with  $\psi$  and the change of these functions at the Morin temperature undoubtedly proves the existence of the magnetic Bragg reflection of X-rays in antiferromagnetic compounds. The origin of these superstructural reflections can only come from the photon-spin interaction. It would be difficult to explain the necessarily vectorial observed effects by any other phenomenon. Furthermore, it is possible with suitable experimental conditions to show that  $P(\psi)$  presents an asymmetry which has been neglected in the results reported above; this asymmetry, related to the cross term  $S_x S_y$ , is characteristic of the magnetic scattering. It is shown by the following experiments.

(2) The effect of the cross term  $S_x S_y$  in  $P(\psi)$  is related to the linear polarization rate

$$\sin^2 2\alpha / (1 + \cos^2 2\alpha)$$

introduced by the monochromator. Both its Bragg angle  $\alpha$  and the polarization rate increase with increasing  $\lambda$  and increasing order of reflection, provided that  $\alpha < 45^\circ$ . Therefore we have first replaced the  $\text{Cu } K\alpha$  radiation ( $\lambda \approx 1.54 \text{ \AA}$ ) with  $\text{Co } K\alpha$  ( $\lambda \approx 1.79 \text{ \AA}$ ) and then used the 004 instead of the 002 reflection of graphite as analyser.

The product  $S_x S_y$  introduces an asymmetry between  $P(\psi)$  and  $P(\psi + 180^\circ)$  because its sign is reversed when the crystal is rotated by  $180^\circ$ , equations (3), (4). For the low-temperature phase  $S_x S_y$  assumes a minimum value at  $\psi = 0^\circ$  and a maximum at  $\psi = 180^\circ$  (Fig. 10). For the high-temperature phase the variation is inverted (maximum at  $\psi = 0^\circ$  and minimum at  $\psi = 180^\circ$ ) and becomes smaller. The experimental and theoretical values of  $P(\psi)$  for different settings of the monochromator are given in Table 1. For the two largest values of the monochromator Bragg angle  $\alpha$  the variations of intensity between  $\psi = 0^\circ$  and  $\psi = 180^\circ$  are large. The value of  $R(\psi)$  at  $\psi = 180^\circ$  is 2.3 times (as against a calculated ratio of 2.54) the value at  $\psi = 0^\circ$  for  $\text{Co } K\alpha$  (Table 1c). This ratio becomes 1.41 (calculated 1.63) for  $\text{Cu } K\alpha$  (Table 1b).

This shows that the cross term produces observable effects. Nevertheless a discrepancy appears between experimental and calculated results, particularly at  $\psi = 0^\circ$  and  $\psi = 180^\circ$ . An error in the polarization rate (the monochromator is not ideally imperfect) may account for only a part of this; the origin of the remaining part is unclear at present.

(3) In order to be sure that the agreement observed between experiment and theory is the same for all the magnetic reflections, we have measured the reflection 101. The radiation used was Co  $K\alpha$  monochromatized by the 002 reflection of graphite and the geometrical conditions were the same as for the measurement of 303; only the  $\theta$  angle was changed. Because of the trigonometric factors in relation (2), the observed integrated intensity is of the same order of magnitude for the 101 and 303 reflections. The  $\theta$  angle of the 101 is small, so that  $P(\psi) \approx S_z^2 \cos^2 \theta$ ; the variations of  $P$  between high and low temperature, and between  $\psi = 0^\circ$  and  $\psi = 90^\circ$  are large (Table 2). The intensities  $I(\psi = 273, 183 \text{ K})$  and  $I(\psi = 363, 298 \text{ K})$ , which should be very small (practically zero), are experimentally observed and also in this case experiment and theory disagree slightly. We have no definite explanation for this; some remaining contribution of multiple scattering is possible, but hardly expected.

## VII. Study of $\text{Fe}_2\text{O}_3$ in magnetic field at room temperature

In the high-temperature phase ( $T > T_M$ ), the weak ferromagnetic moment lies in the (001) plane and is perpendicular to the direction of the antiferromagnetic spins. Because the anisotropy in the (001) plane is negligible, a magnetic field along this plane tends to align the ferromagnetic moments along itself while the antiferromagnetic are perpendicular to this field. If the field is moderately high the crystal becomes single domain and the magnetization saturates (Nathans *et al.*, 1964). On the contrary, a field lower than  $1 \text{ A m}^{-1}$

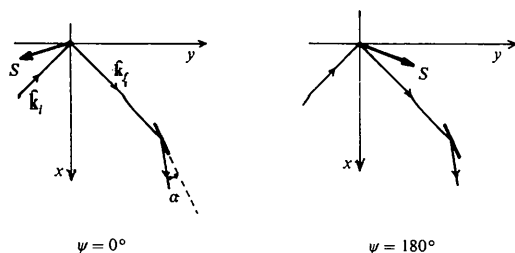


Fig. 10. The low-temperature spin direction with respect to the  $x$  and  $y$  axes, at  $\psi = 0^\circ$  and  $\psi = 180^\circ$ . Changes in intensity between  $\psi = 0^\circ$  and  $\psi = 180^\circ$  are due to the polarization introduced by the monochromator placed between the sample and the detector ( $\alpha$  = angle of reflection).

Table 1.  $P(\psi)$  and  $R(\psi)$  for some wavelengths and some orders of diffraction by the monochromator; pol is for polarization rate

(a)  $\lambda(\text{Co } K\alpha)$ ; 002 graphite;  $\alpha = 15.50^\circ$ ; pol. = 0.153.

$\psi$	$0^\circ$		$180^\circ$		$73^\circ$	
	exp.	theor.	exp.	theor.	exp.	theor.
$P(\psi, 298 \text{ K})$	$0.34 \pm 0.01$	0.39	$0.31 \pm 0.01$	0.37	$0.25 \pm 0.01$	0.24
$P(\psi, 183 \text{ K})$	$0.26 \pm 0.01$	0.22	$0.28 \pm 0.01$	0.25	$0.53 \pm 0.01$	0.51
$R(\psi)$	0.76	0.56	0.90	0.67	2.12	2.12

(b)  $\lambda(\text{Cu } K\alpha)$ ; 004 graphite;  $\alpha = 27.37^\circ$ ; pol. = 0.50.

$\psi$	$6^\circ$		$174^\circ$	
	exp.	theor.	exp.	theor.
$P(\psi, 298 \text{ K})$	$0.38 \pm 0.01$	0.41	$0.38 \pm 0.01$	0.37
$P(\psi, 183 \text{ K})$	$0.22 \pm 0.01$	0.17	$0.31 \pm 0.01$	0.25
$R(\psi)$	0.58	0.41	0.82	0.67

(c)  $\lambda(\text{Co } K\alpha)$ ; 004 graphite;  $\alpha = 32.28^\circ$ ; pol. = 0.69.

$\psi$	$0^\circ$		$180^\circ$		$73^\circ$	
	exp.	theor.	exp.	theor.	exp.	theor.
$P(\psi, 298 \text{ K})$	$0.33 \pm 0.01$	0.42	$0.23 \pm 0.01$	0.34	$0.29 \pm 0.02$	0.26
$P(\psi, 183 \text{ K})$	$0.17 \pm 0.01$	0.15	$0.27 \pm 0.01$	0.32	$0.41 \pm 0.01$	0.44
$R(\psi)$	0.51	0.37	1.17	0.94	1.41	1.69

Table 2.  $P(\psi)$ ,  $R(\psi)$  and  $D(\psi)$  for the 101 magnetic reflection

$\psi$	$3^\circ$		$85^\circ$	
	exp.	theor.	exp.	theor.
$P(\psi, 298 \text{ K})$	$0.50 \pm 0.015$	0.48	$0.19 \pm 0.01$	0.08
$P(\psi, 183 \text{ K})$	$0.13 \pm 0.01$	0.04	$1 \pm 0.03$	0.85
$R(\psi)$	0.26	0.08	5.26	11.33
$D(\psi)$	-0.37	-0.44	0.81	0.77

in the direction of the  $c$  axis has no effect because the anisotropy in a plane containing  $c$  is large. By magnetic measurements, we have verified that a field of a few tenths  $\text{A m}^{-1}$  within the (001) plane was sufficient to saturate our crystal and that a field of  $1 \text{ A m}^{-1}$  parallel to  $c$  changed very slightly its magnetization.

An electromagnet set on the goniometer gives a field  $H$ , whose maximum value is  $0.17 \text{ A m}^{-1}$ , directed along  $x$ ,  $y$  or  $z$  according to different pole pieces (for  $H$  along  $x$ , a hole was made for the sample holder in one of the pole pieces). We have measured the integrated intensity of the 101 magnetic reflection at  $\psi = 0^\circ$  (Fig. 5), *i.e.* with the (001) plane perpendicular to the diffraction plane, while applying successively:

(1) A magnetic field  $H \approx 0.1 \text{ A m}^{-1}$  in the  $c$  direction. In this case the intensity of 001 does not change, which is due to the high anisotropy in a plane containing  $c$ .

(2) A magnetic field  $H_x$ , which tends to orientate the ferromagnetic moment along  $x$ , and thus the antiferromagnetic ones along  $z$ . We have observed an increase in the intensity of the 101 reflection. The variation of  $P(\psi = 0^\circ)$  as a function of  $H_x$  is reported in Fig. 11. The observed saturation value  $P = 0.95$  is equal to the value calculated in the hypothesis of a single domain with antiferromagnetic moments along  $z$ .

(3) A magnetic field  $H_z$ , which tends to orientate the antiferromagnetic moments within the (001) plane, along the  $a^*$  axis, which is close to the  $x$  axis (Fig. 5).

We have observed a decrease of the intensity of the 101 reflection. The curve  $P(\psi = 0^\circ)$  as a function of  $H_z$  is reported in Fig. 11. The value calculated in the hypothesis of a single domain, with antiferromagnetic moments oriented along  $x$ , is  $P(\psi = 0^\circ) \simeq 0$  which disagrees with the experimental value 0.23. One should notice that X-rays see only the surface of the sample (some microns); the presence of some anomalous anisotropy in this region may be suspected.

## VII. Conclusion

These experiments show, beyond doubt, that the magnetic superstructural Bragg reflections in antiferromagnetic compounds can be observed and that they can be calculated by taking into account the photon-spin interaction (paper I). These reflections are measur-

able with a conventional X-ray tube (power  $\simeq 1$  kW) since in  $\text{Fe}_2\text{O}_3$  the intensity, at the peak of some reflections, is as high as  $200 \text{ counts min}^{-1}$ . However the use of a high-intensity X-ray tube would allow a reduction in measurement time or in crystal dimension. Disagreements between the theoretical intensities and some of the experimental ones remain to be explained; their order of magnitude is 10 to 20% of the maximum values. Experimental difficulties related to multiple scattering and eventual anomalies of the magnetic anisotropy near the surface of the sample are two possible reasons.

As the interaction between photon X and spin has a more complicated form than the one between neutron and spin, this technique could be used, in some cases, in addition to neutron diffraction, to complement the information concerning the direction of atomic moments. X-rays could also be used to study compounds which have a large absorption cross section for neutrons, for instance compounds containing gadolinium. Because of the short penetration depth of X-rays in all materials, by this technique one can see magnetic effects near the surface, or in thin materials.

We are indebted to L. Blond and C. Mouget for technical assistance, M. Chabre for the design of the mirror and P. Mollard and B. Foulleux for the magnetic measurements.

## References

- BERGEVIN, F. DE & BRUNEL, M. (1972). *Phys. Lett. A*, **39**, 141–142.
- BERGEVIN, F. DE & BRUNEL, M. (1981). *Acta Cryst. A* **37**, 314–324.
- BLAKE, R. L., HESSEWICKS, R. E., ZOLTAI, T. & FINGER, L. W. (1966). *Am. Mineral.* **51**, 123–129.
- BROCKHOUSE, B. N., CORLISS, L. M. & HASTINGS, J. M. (1955). *Phys. Rev.* **98**, 1721–1727.
- COLE, H., CHAMBERS, F. W. & DUNN, H. M. (1962). *Acta Cryst.* **15**, 138–144.
- DZIALOSHINSKY, I. (1958). *Phys. Chem. Solids*, **4**, 241–255.
- FLANDERS, P. J. & REMEIK, J. P. (1965). *Philos. Mag.* **11**, 1271–1288.
- NATHANS, R., PICKART, S. J., ALPERIN, H. A., BROWN, P. J. (1964). *Phys. Rev.* **136**, A 1641–A 1647.
- SHULL, C. G., STRAUSSER, W. A. & WOLLAN, E. O. (1951). *Phys. Rev.* **83**, 333–345.

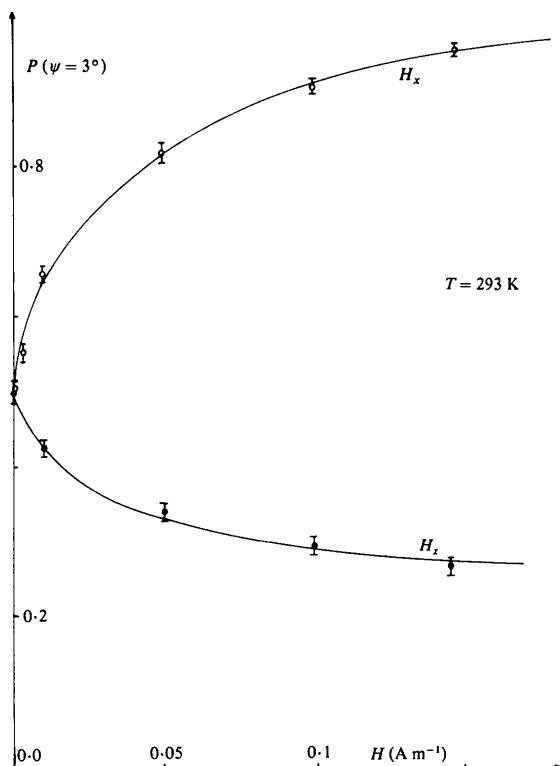


Fig. 11. Variations of the intensity of the 101 magnetic reflection in applied fields  $H_x$  and  $H_z$ .